Latent thermal energy storage system for heat recovery: numerical study

S. Rigal[a], D. Haillot[a], S. Gibout[a], E. Franquet[a] and J.P. Bédécarrats[a]

[a] Univ. Pau & Pays Adour, EA 1932-LaTEP-ENSGTI, Pau, France, sacha.rigal@univ-pau-fr **(CA)**

Abstract:

The continuous increase in the level of greenhouse gas emissions and the rise in fuel prices are the main driving forces to encourage all stakeholders in the energy sector to improve the efficiency of the systems. A large amount of energy is rejected by the industry at low temperature level (between 0 and 150 °C). Indeed, considering all the industrial processes in France, the amount of energy lost in this temperature range is estimated at 75 TWh/year.

Storage of heat is one of the major issues to bridge the gap between energy supply and demand. The thermal energy storage (TES) technology including phase change materials (PCM) appears particularly attractive in this specific application. This solution is attractive since it provides a high energy storage density and has the capacity to store heat as latent heat of fusion at a constant temperature corresponding to the phase change transition temperature of the PCM (in the case of pure substances). These parameters are especially suitable for heat recovery in industrial processes in which there is a delay between the process step at which the energy is lost and the process step at which this energy could be recovered.

The general objective of our work is to propose a design of a TES system dedicated to the kind of applications detailed above. This paper describes a numerical study on a future experimental pilot composed of a cylindrical tank filled with encapsulated PCM. This model investigates the influence of various parameters on the charge mode. Among the studied parameters, the thermal conductivity of the PCM and the diameter of the capsule are significant parameters on the storage mode. An increase in the PCM thermal conductivity and a decrease in the capsule diameter increase the storage power.

Keywords:

Latent thermal energy storage, Heat recovery, Numerical model, Phase Change Material.

INTRODUCTION

With the increasing demand for industrial produce, the trend is on reducing energy consumption by increasing energy efficiency. Among the various possibilities to achieve such a goal, one solution is to save energy by re-using the heat released all along the process. Nowadays, high grade thermal energy (> 400°C) is typically recovered, whereas lower grade heat is often rejected to the environment [1]. Indeed, considering all the industrial processes in France, the amount of energy lost in the temperature range below 150 °C is estimated to 75 TWh / year. It represents more than 18% of the primary energy consumption by the industry.

In a large number of industrial processes, there is a time delay between the process step at which the energy is lost and the process step at which this energy could be recovered. Waste heat recovery and thermal energy storage technologies seem to be the best solution to match the energy supply with the energetic demand due to this fluctuating phenomenon of energy sources. By utilizing waste heat, thermal energy storage systems can reduce the consumption of limited fossil fuel reserves and restrain output of CO_2 to preserve the environment [2].

Thermal energy storage can be broken up into three major classifications based on the principle of the energy storage method: sensible heat storage, latent heat storage and chemical heat storage. Although thermochemical storage systems provide promising advantages, the corresponding storage materials are still too expensive and this solution is, at the present time, at early stages of development [3]. Latent heat storage using phase change materials (PCM) is one of the most attractive solutions because it provides high thermal energy storage densities at constant temperature over a wide range of applications from sub-zero to very high temperature systems [4]. Indeed, as a new type of energy-

conserving and environment-friendly material, PCMs utilize latent heat of the melting/solidification process to store energy.

However, most of PCMs have a low thermal conductivity, leading to low charging and discharging rates. By encapsulating the PCM into capsules, the surface area over which heat transfer occurs is increased and thus the charging and discharging times of the system are decreased. Moreover, some PCMs have their own drawbacks (supercooling or segregation) and the encapsulation can reduce such problems [5].

Researchers have been interested in the encapsulation of the PCM in different capsules as sphere, cylinder, plate or tube for investigating the effects of geometrical configurations.

Primarily works have been realized in the case of a cold storage. Arnold [6] and Ismail and Henriquez [7] studied the melting and freezing processes of water as PCM in spherical capsules thanks to a series of charging and discharging experiments. Tieyi et al. [8] have investigated a system in which the cool storage tank is filled with rectangular cases containing the PCM. With a numerical model, they studied the effects of different parameters such as the flow rate or the supercooling, and then, they compared the obtained results with available literature experimental data. Bedecarrats et al. [9] studied numerically an ice storage tank using spherical capsules, taking into account the supercooling phenomenon during the solidification of water. The effects of the coolant flow rate, the inlet temperature and the position of the tank (horizontal or vertical) have also been discussed in their study. Chen et al. [10-13] developed a general lump model to predict the thermal performance of a low temperature storage system during the solidification process, utilizing cylindrical capsules with varying inlet coolant temperature and flow rate. Kousksou et al. [14] investigated the influence of supercooling and the position of storage tank with to a two-dimensional model. Results show that the optimum running charging mode is obtained in the case of vertical position, where the motion due to natural convection is in the same direction as the forced convection.

More recently, authors started to study higher temperatures thermal storage for two main applications.

The first one is for domestic hot water system or for space heating applications (temperature range below 65 °C). De Gracia et al. [15] explore numerically the heat transfer during charge and discharge in a typical domestic hot water cylinder in which the PCM is encapsulated in 57 vertical pipes. Jradi et al. [16] presented a detailed mathematical model for the transient behaviour of rectangular macro-encapsulated PCM in both melting and freezing phases in the temperature range of 30 °C.

The second application is for concentrated solar power plants (temperature range above 300 °C). Zhao et al. [5] conducted heat transfer analysis for high melting temperature encapsulated phase change materials capsules containing sodium nitrate as PCM with a melting point at 308 °C. Two-dimensional transient heat transfer simulation is applied to different sizes and geometries of capsules using different types of heat transfer fluids at various flow conditions. Zhang et al. [17] illustrate the results obtained when encapsulating $NaNO_3/KNO_3$ PCM in a tube, as example of heat storage application using a multi tubular exchanger filled with PCM, and make a comparison between experimental results and theoretical predictions in terms of achieved discharging rates. Elmozughi et al. [18] and Solomon et al. [19] have examined the effect of an internal air void on the heat transfer phenomenon within encapsulated PCM. They simulated heat transfers on a two dimensional cylindrical capsule using sodium nitrate as the high temperature PCM, with different boundary conditions and thanks to a volume of fluid method (VOF).

This paper focus on a thermal energy solution in a new range of temperature (around 150°C) which is, as previously mentioned, particularly adapted to a broad range of industrial waste heat recovery. The objective is to investigate numerically the effects of different parameters on the performance of a packed bed latent heat thermal energy storage system consisting of spherical capsules in a cylindrical storage tank. The effects of the thermal characteristics of the PCM (enthalpy of fusion, density and thermal conductivity), PCM encapsulation material (diameter, thickness, thermal conductivity) have been discussed. In this study, only the charging process is considered (melting of the PCM).

1. Numerical Analysis

Fig. 1 shows the layout of the physical system that has been investigated. It is composed of a cylindrical tank of height *H* and diameter *D* filled with spherical capsules containing PCM (Fig. 1(a)). Main assumptions are as follows:

- The tank is fully insulated;
- The flow in the tank is axial and incompressible;
- The temperature only varies along the axial direction;
- The tank height is divided into M layers (Fig. 1(b)) of sufficiently small length so that the layer can be assumed to be at a single temperature;
- Heat transfer conduction between spherical capsules in contact is negligible;
- Kinetic and potential energy changes are negligible.

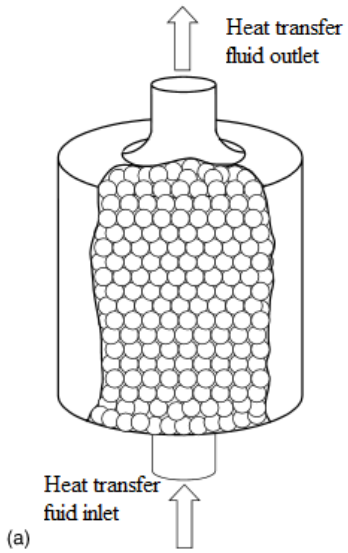

Fig. 1a. Layout of the storage system. Adapted from [7].

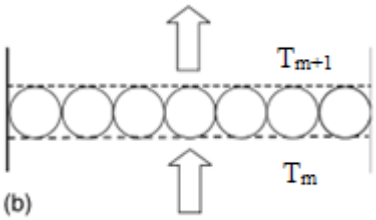

Fig. 1b. Energy balance over a layer of spherical capsules. Adapted from [7].

The packed bed is divided into several elements, each containing *N* PCM capsules surrounded by the heat transfer fluid. The following equations are directly inspired from a previous paper of our laboratory [9]. This work initially used and validated for low temperature energy storages (below 0°C) has been adapted to our new application, medium temperature industrial waste heat recovery.

The first principle of thermodynamics (law of conservation of energy) in transient state is written for each element of the tank. The modelling is based on Finite Volume Method.

The energy balance on the layer M leads to:

$$\rho_f C_f V \frac{dT}{dt} = \rho_f C_f q_v (T_m - T_{m+1}) + \sum_{i=1}^{N} \phi_i \qquad (1)$$

Where *N* is the number of spheres in the layer, ϕ_i are the heat fluxes between each spherical capsule and the working fluid. *T* is the temperature at the center of the layer and corresponds to the average of T_m and T_{m+1}, the boundary temperatures of the mesh. *V* is the volume occupied by

the fluid in the layer, ρ_f is the density of the fluid and C_f its specific heat and q_v is the fluid volume flow rate.

Spherically symmetrical melting is assumed inside a nodule Fig. 2. It is supposed that the melting process begins on the inner surface of the polyethylene envelope and after the solid melts concentrically to the center. As soon as the melting begins, the solid is at the melting temperature T_M.

It is evident that when the process starts, the melting occurs equally over the inner surface of the nodule envelope, but as soon as there is a significant amount of liquid, buoyancy forces, due to density differences between solid and liquid phase, cause the solid phase to move and gravitate to the bottom of the nodule (selected PCMs have a higher density for the solid phase than for the liquid one). It has been revealed that the internal convection during melting has to be taken into account. In order to simplify the model, the presence of natural convection in the liquid phase is taken into account using an effective thermal conductivity of the liquid phase which is higher than the real liquid conductivity k_l. Thus, the melting process is analyzed as a pure heat conduction problem.

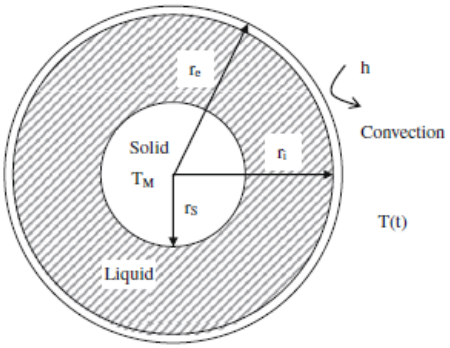

Fig. 2. Melting inside a spherical capsule. Adapted from [9].

Considering the spherical capsule shown in Fig. 2, the heat transfer flux during the melting process is:

$$\phi_i(t) = \frac{T_M - T(t)}{\frac{1}{hS} + \frac{1}{4\pi k_p}\left(\frac{1}{r_i} - \frac{1}{r_e}\right) + \frac{1}{4\pi k_l}\left(\frac{1}{r_S} - \frac{1}{r_i}\right)} \quad (2)$$

With k_p the thermal conductivity of the nodule envelope, h the heat transfer coefficient between the envelope and the heat transfer fluid, S the external surface of the envelope and T_M the melting temperature of the PCM and r_s the radius of the solid PCM.

The determination of the heat transfer fluid coefficient h is done by using Equation (3) [9]:

$$N_u = \frac{hD}{k_f} = C^{st} Pr^{1/3} Re^{1/2} \quad (3)$$

Where D is the external diameter of the nodule, C^{st} a coefficient estimated at 1 in our case [9], k_f the thermal conductivity of the heat transfer fluid, Re the Reynolds number and Pr the Prandtl number.

The temperature of the PCM inside the nodule $\theta(r,t)$ can be calculated thanks to the quasistationary approximation.

$$\theta(r,t) = T_M + [T(t) - T_M]\frac{1 - \frac{r_s(t)}{r}}{\left(\frac{k_l}{k_p} - 1\right)\frac{r_s(t)}{r_i} + \left(\frac{k_l}{hr_e} - \frac{k_l}{k_p}\right)\frac{r_s(t)}{r_e} + 1} \quad (4)$$

Before and after the complete phase change, it is assumed that the temperatures of the solid and liquid phases inside the nodule are homogeneous, and the internal energy variation in the PCM is equal to the flux exchanged by the nodule. Consequently when the PCM is completely liquid

(before the melting), with V_n the volume of PCM inside a nodule, the heat flux inside a spherical capsule is determined by the following equations:

$$\rho_L C_L V_n \frac{dT_L(t)}{dt} = -\phi_L \quad (5)$$

With:

$$\phi_L(t) = \frac{T_L - T(t)}{\frac{1}{hS} + \frac{1}{4\pi k_p}\left(\frac{1}{r_i} - \frac{1}{r_e}\right)} \quad (6)$$

2. Numerical results

In the present work, a cylindrical storage tank of 0.4 m diameter and 0.8 m height, completely filled (ratio volume of nodule over volume of the tank equals to 60.6 %) with 130 PCM capsules of 90 mm in diameter and 2 mm in thickness has been considered. This tank corresponds to an experimental pilot that had been designed in our laboratory and will be tested in the near future. It can be considered that the used PCM melts at the temperature of 150 °C. The initial and final temperatures of the tank are respectively 140 °C and 160 °C. The flow rate of the heat transfer fluid is 0.25 $m^3.h^{-1}$ and the heating rate of the fluid is 5 °C h^{-1}.

As the temperature of the heat transfer fluid is about 150 °C, stainless steel was chosen as container material with a thermal conductivity of 7.7 W m^{-1} K^{-1} according to [20].

Numerical calculations were done for various conditions in order to investigate the effects of different parameters on the charging process (melting of the PCM). First, the two main families of PCM (organics and inorganics) have been compared, taking into account an average of their thermal properties. Then, the effects on the performance of the packed bed, of different thermal conductivities of the PCM, different conductivities of the shell of the capsule and different sizes and thicknesses of the nodule have been investigated.

2.1. Comparison of the families of PCMs

In Table 1, the main thermal properties of the two families of PCM are summarized: the latent heat of fusion, the thermal conductivity and the density. It is considered that their specific heat is equal to 2.0 kJ kg^{-1} K^{-1}. In order to compare each of these PCM families, numerical simulations have been performed with these respective thermal properties. Results are presented in Fig. 3.

Table 1. Average thermal properties of the mains PCM families. Adapted from [21 and 22].

Property	*Organic*	*Inorganic*
Latent heat of fusion (kJ kg^{-1})	190	230
Thermal conductivity (W m^{-1} K^{-1})	0.20	0.52
Density (kg m^{-3})	800	1600

Fig. 3(a) shows the evolution of the inlet and outlet temperature of the tank for each PCMs family. The thermal storage is achieved when the outlet temperature has reached the temperature imposed at the inlet. It is observed that the storage is faster in the case of the organics.

Fig. 3(b) below shows the evolution of the energy stored in the tank for the two different subdivisions of PCMs. According to this figure, it can be noticed that the storage time and the quantity of energy stored increase with the increase in storage density per unit volume (which is the product of the density by the latent heat). Thus the energy stored is maximal for inorganic PCMs.

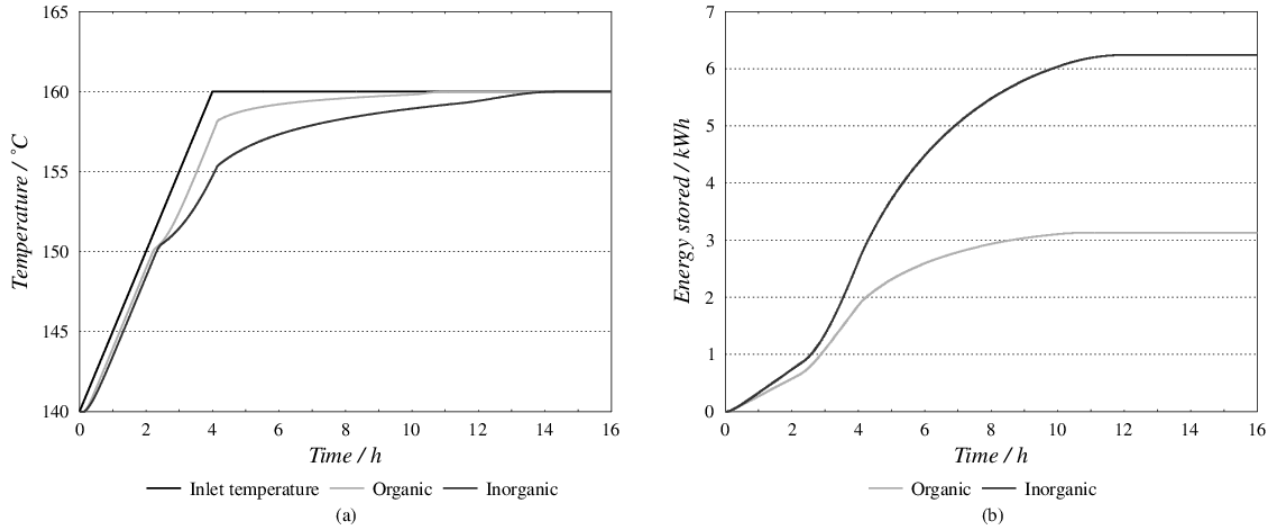

Fig. 3. Comparison of different families of PCMs: (a) inlet and outlet temperatures, (b) energy stored.

To conclude, the time to store 99 % of the total energy, the stored energy and the power for each PCM subdivision have been determined. Results are summarized in Table 2.

Table 2. Comparison on the storage for different families of PCMs

Family	*Time to store 99 % of the energy (h)*	*Energy stored (kWh)*	*Storage power (kW)*
Organic	9.9	3.1	0.313
Inorganic	10.3	6.2	0.602

To compare to the performances of the storage, the storage power has been defined as the ratio of the energy stored and the time to store 99 % of this energy.

It can be seen that, with the considered values of thermal properties, the inorganics are the ones which store the energy with the most effective way (energy stored and storage power is higher compared to organic materials).

According to the results, for the following simulations the use of the thermal properties corresponding to the family of the inorganics PCM has been chosen.

2.2. Effect of the thermal conductivity of the PCM

In this section the thermal conductivity of the capsule has been fixed at a value of 7.7 W m^{-1} K^{-1} (corresponding to stainless steel) and the thermal conductivity of the PCM was varied from k_l, the initial conductivity of the liquid phase, to hundred times this value. Indeed some previous works have shown that adding expanded natural graphite [23] or metallic compound [24] to the PCM could increase significantly the initial low thermal conductivity of the material. The PCM thermal conductivity is now written k_{eff}.

Fig. 4 shows the evolution of the inlet and outlet temperature of the tank and the energy stored in the tank, for different thermal conductivities of the PCM.

In Fig. 4(a) it can also be noticed that the duration of the storage decreases with the increase in thermal conductivity of the PCM. The higher the thermal conductivity is, the shorter the time interval needed for reach the final inlet temperature.

Fig. 4(b) shows the influence of the thermal conductivity of the PCM on the time to store the whole energy inside the tank. The higher the thermal conductivity is, the faster the storage of energy is. It can also be noticed that between k_{eff} and 10*k_{eff}, the time of storage decreases significantly. It can also

be noticed that above 10*k_{eff}, an increase in the thermal conductivity decreases slightly the time of storage.

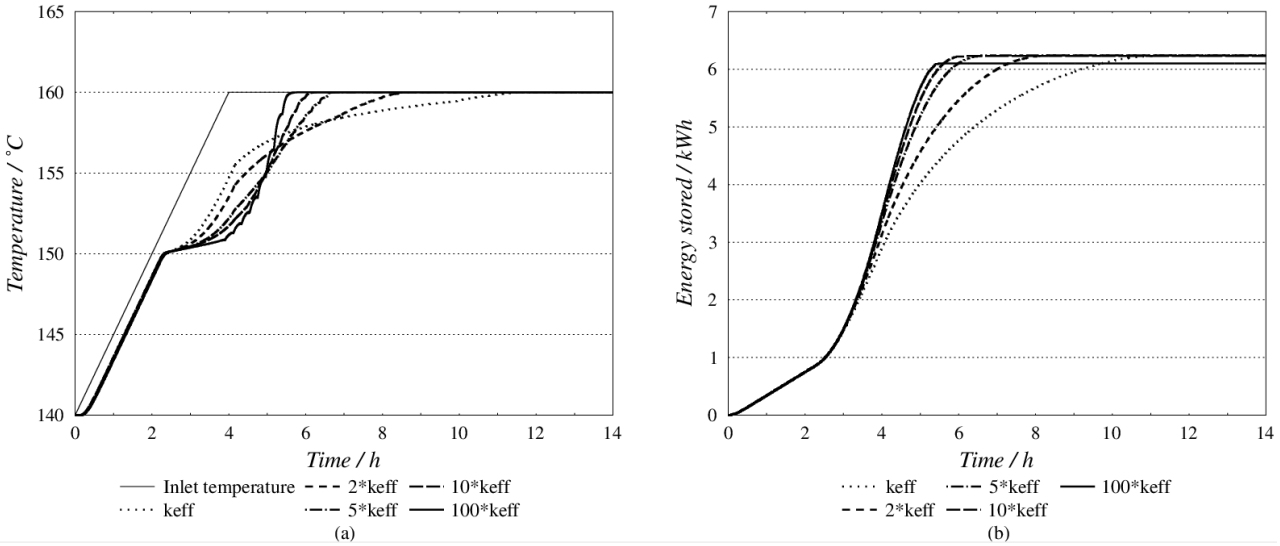

Fig. 4. Comparison of different conductivities of the PCM: (a) inlet and outlet temperatures, (b) energy stored versus time.

In Table 3, the results of the effect of different thermal conductivities of the PCM are listed.

Table 3. Comparison on the storage for different thermal conductivities of the PCM

Thermal conductivity	*Time to store 99 % of the energy (h)*	*Energy stored (kWh)*	*Storage power (kW)*
$k_{eff} = k_l$ (0.52 W m^{-1} K^{-1})	10.3	6.2	0.602
2*k_{eff} (1.04 W m^{-1} K^{-1})	7.7	6.2	0.803
5*k_{eff} (2.6 W $m^{-1}K^{-1}$)	6.2	6.2	0.996
10*k_{eff} (5.2 W m^{-1} K^{-1})	5.7	6.2	1.081
100*k_{eff} (52 W m^{-1} K^{-1})	5.3	6.2	1.139

With the increase in the thermal conductivity, it can be observed that the time to store 99 % of the total energy is 1.9 time shorter when the thermal conductivity is ten time larger, and 2.0 time shorter when the thermal conductivity is 100 time larger.

2.3. Effect of the thermal conductivity of the nodule

In this section, the thermal conductivity of the PCM is fixed at 0.52 W m^{-1} K^{-1} and the thermal conductivity of the wall of the nodule was varied, taking different values according to [20] (see Table 4). Fig. 5 shows the evolution of the inlet and outlet temperatures and the energy stored in the tank, for different thermal conductivities of the shell of the capsule.

Fig. 5(a) and 5(b) show that the influence of the thermal conductivity of the nodule is negligible in this case on the storage power.

In Table 4 the results of the effect of different thermal conductivities of the shell of the capsule are listed.

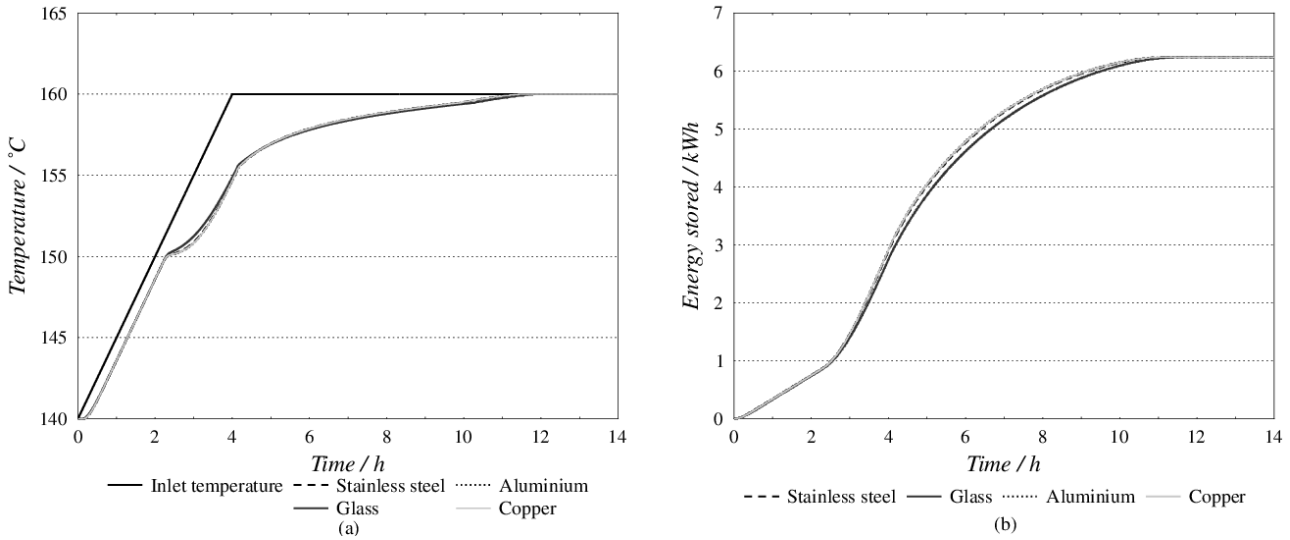

Fig. 5. Comparison of different conductivities of the nodule: (a) inlet and outlet temperatures, (b) energy stored versus time.

Table 4. Comparison on the storage for different thermal conductivities of the nodule

Material	*Thermal conductivity ($W\ m^{-1}\ K^{-1}$)*	*Time to store 99 % of the energy (h)*	*Energy stored (kWh)*	*Storage power (kW)*
Stainless steel	7.7	10.3	6.2	0.602
Glass	0.78	10.6	6.2	0.583
Aluminium	204	10.3	6.2	0.604
Copper	386	10.3	6.2	0.604

It can be observed that, the effect of the variation of the thermal conductivity of the shell of the nodule does not play an important role here. Indeed, for a higher conductivity of the shell, the time to store 99 % of the whole energy is just the same. According to Equation (2), it can be thought that the thermal resistance due to the thermal conductivity of the PCM is too large compared to the one of the nodule wall and makes the variation of the thermal conductivity of the nodule wall ineffective.

2.4. Effect of the size of the nodule

In the following section the effect of the size of the nodule on the inlet and outlet temperatures of the tank and on the energy stored (Fig. 6(a) and 6(b)) has been investigated.

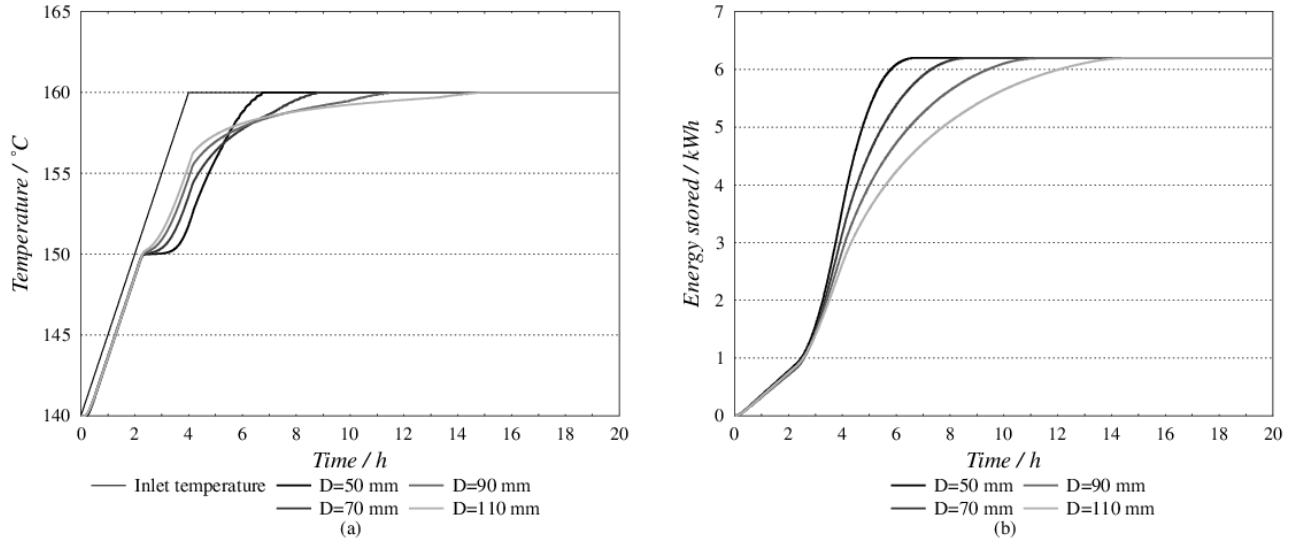

Fig. 6. Comparison of different sizes of the nodule: (a) inlet and outlet temperatures, (b) energy stored versus time.

To carrying out the simulations, the thermal conductivity of the PCM has been fixed at the value of k_{eff} = 0.52 W m^{-1} K^{-1} and the thermal conductivity of the nodule wall is equal to k_p = 7.7 W m^{-1} K^{-1}.

In Fig. 6(a) the appearance of a "plateau" near the melting temperature for the smallest nodules can be noticed.

The influence of the diameter of the nodule on the time to store the whole energy inside the tank is clearly visible in Fig. 6(b). The smaller the diameter of the capsule is, the shorter the time to store the energy is.

In Table 5, the main results of the effect of the size of the nodule have been listed.

Table 5. Comparison on the storage for different size of the nodule

Diameter of the nodule (mm)	*Time to store 99 % of the energy (h)*	*Energy stored (kWh)*	*Storage power (kW)*
110	13.3	6.2	0.467
90	10.3	6.2	0.602
70	7.9	6.2	0.787
50	6.2	6.2	1.005

A slightly decrease on the time to store the total energy inside the tank is noted, when the diameter of the nodule decreases even if the energy stored is the same. By comparing the nodules of diameter 110 mm and diameter 50 mm, an increase of 115 % of the power storage is noted. This is due to the increase in the exchange surface between the heat transfer fluid and the PCM.

2.5. Effect of the thickness of the capsule

Here, the effects of different thicknesses of the nodule wall on the temperatures of the tanks (Fig. 7(a)) and on the energy stored inside the tank (Fig. 7(b)) have been compared. The parameters of the nodule and the PCM were fixed with k_{eff} = 0.52 W m^{-1} K^{-1}, the thermal conductivity of the PCM, k_p = 7.7 W m^{-1} K^{-1} the thermal conductivity of the shell of the capsule and D = 90 mm the diameter of the nodule.

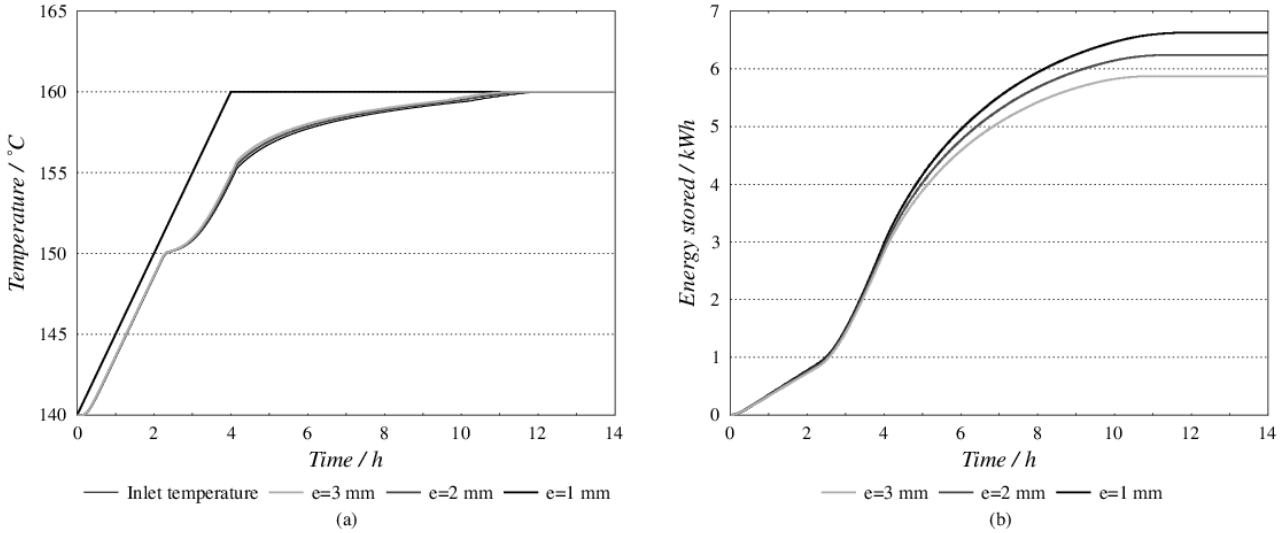

Fig. 7. Influence of the thickness of the nodule envelope: (a) inlet and outlet temperatures, (b) energy stored versus time.

On Fig. 7(a), the interval time to reach the final inlet temperature seems to be equal for each thickness of the nodule. The only difference that can be noted, is the early changes in temperature of the PCM when the thickness is larger. This is because there is less PCM inside the nodule and this reason explains the curves Fig. 7(b) where a decrease in the total energy stored inside the nodule is noted.

Table 6 lists the values for various thicknesses of the nodule.

Table 6. Comparison on the storage for different thicknesses of the nodule

Thickness of the nodule envelope (mm)	*Time to store 99 % of the energy (h)*	*Energy stored (kWh)*	*Storage power (kW)*
3	10.6	5.9	0.593
2	10.3	6.2	0.602
1	9.8	6.6	0.619

As it has been assumed in Fig. 7, the time to reach the final inlet temperature and therefore the time to store the whole energy inside the tank is quite equal in the different cases. The main difference lies in the energy stored inside the tank. Between a thickness of 1 mm and a thickness of 3 mm the gain of the energy storage is around 5 %. Consequently, for the same duration of storage, the storage power is increased of 5 %.

Conclusion

In the present study, a packed bed latent heat thermal energy storage has been analysed numerically to predict the thermal behaviour of the system. The studied system corresponds to an experimental facility that will be designed and built in our laboratory for experimental testing in the near future. This paper investigates the influence of various parameters on the charge mode as the type of PCM and its thermal conductivity, the thermal conductivity of the shell of the capsule, its size and its thickness. The following conclusions can drawn from the results:

a) The thermal conductivity of the PCM is a significant parameter on the storage power. By comparing a PCM with a thermal conductivity of 0.52 W m^{-1} K^{-1} and the same PCM with a conductivity ten times higher, it was shown that the storage power was 1.8 times higher. However it has been noticed that beyond this value, the increase in the thermal conductivity no longer significantly reduces the time of storage.
b) The thermal conductivity of the nodule envelope has a low influence on the results.
c) The charge rate is higher for the nodule of smaller radius compared those of larger radius.
d) By changing the thickness of the wall nodule, the volume of PCM inside the capsule has been changed also and consequently the total energy stored is higher when the thickness is lower. Moreover it has been noticed that the time to store the whole energy was quite equal in the different cases, thus, the charging rate is higher for the nodule of smaller thickness.

Acknowledgments

This work was carried out through the STEEP project (Thermal Storage for eco efficiency industial processes) funded by the 2013 ANR-SEED program of the French National Research Agency (project "ANR-13-SEED-0007").

Nomenclature

C Specific heat of the fluid (J K^{-1})
C^{st} Coefficient number for the Nusselt formula
D Diameter (m)
e Thickness of the envelope (m)
h Heat exchange coefficient between the envelope and the heat transfer fluid (W m^{-2} K^{-1})
H Height of the tank (m)
k_{eff} Effective thermal conductivity of the PCM (W m^{-1} K^{-1})
k_f Thermal conductivity of the working fluid (W m^{-1} K^{-1})

k_p Thermal conductivity of the envelope (W m^{-1} K^{-1})

N Number of nodules in a mesh

Nu Nusselt number

Pr Prandtl number

q_v Fluid volume flow rate (m^3 s^{-1})

Re Reynolds number

r_e External radius of the nodule (m)

r_i Internal radius of the nodule (m)

r_s Radius of the solid PCM (m)

S External surface of the nodule (m^2)

T Temperature (K)

V Volume of the layer (m^3)

V_n Volume of the PCM inside one nodule (m^3)

Greek symbols

ϕ Heat flux exchange between the working fluid and spherical capsule (W)

ρ Density of the fluid (kg m^{-3})

θ PCM temperature (K)

Subscripts

f heat transfer fluid

L liquid

M melting

S solid

References

[1] BCS Incorporated, 2008. Waste heat Recovery : Technologies and opportunities in US Industries, U.S. Department of Energy, Industrial Technologies Program. Available at: <https://www1.eere.energy.gov/manufacturing/intensiveprocesses/pdfs/waste_heat_recovery.pdf> [accessed 22.4.2014]

[2] Anisur M.R., Mahfuz M.H., Kibria M.A., Saidur R., Metselaar I.H.S.C., Mahlia T.M.I., 2013. Curbing global warming with phase change materials for energy storage. Renewable and Sustainable Energy Reviews 18, 23–30.

[3] Nithyanandam K., Pitchumani R., Mathur A., 2014. Analysis of a latent thermocline storage system with encapsulated phase change materials for concentrating solar power. Applied Energy 113, 1446–1460.

[4] Karkri M., Lachheb M., Nógellová Z., Boh B., Sumiga B., AlMaadeed M.A., Fethi A., Krupa I., 2015. Thermal properties of phase-change materials based on high-density polyethylene filled with micro-encapsulated paraffin wax for thermal energy storage. Energy and Buildings 88, 144-152.

[5] Zhao W., Elmozughi A.F., Oztekin A., Neti S., 2013. Heat transfer analysis of encapsulated phase change material for thermal energy storage. International Journal of Heat and Mass Transfer 63, 323–335.

[6] Arnold D., 1990. Dynamic simulation of encapsulated ice stores. Part I: the model. ASHRAE Trans 96(1):1103–1110

[7] Ismail K.A.R., Henriquez J.R., 2002. Numerical and experimental study of spherical capsules packed bed latent heat storage system. Applied Thermal Engineering; 22:1705–16.

[8] Tieyi G., Yinping Z., Xinshi G., 1996. Theoretical analysis of heat transfer in a cool storage tank filled with rectangular enclosures containing phase change material, Buxuan W., Heat Transfer Science and Technology, 734 - 739, Higher Education Press, Beijing, China

[9] Bédécarrats J.P., Castaing-Lasvignottes J., Strub F., Dumas J.P., 2009. Study of a phase change energy storage using spherical capsules. Part II: numerical modelling. Energy Convers. Manage.; 50:2537–46.

[10] Chen S.L., Yue J.S., 1991. A simplified analysis for cold storage in porous capsules with solidification. ASME J Energy Resour Technol 113:108–116

[11] Chen S.L., Yue J.S., 1991. Thermal performance of cool storage in packed capsules for air conditioning. Heat Recov Syst CHP 11(6):551–561

[12] Chen S.L., 1992. One dimensional analysis of energy storage in packed capsules. ASME Journal of Solar Energy Engineering; 114:127–30.

[13] Chen S.L., Chen C.L., Tin C.C., Lee T.S., Ke M.C., 2000. An experimental investigation of cold storage in an encapsulated thermal storage tank. Exp Therm Fluid Sci 23:133–144

[14] Kousksou T., Bedecarrats J.P., Dumas J.P., Mimet A., 2005. Dynamic modeling of the storage of an encapsulated ice tank. Appl Therm Eng 25:1534–1548

[15] De Gracia A., Oró E., Farid M.M., Cabeza L.F., 2011. Thermal analysis of including phase change material in a domestic hot water cylinder. Applied Thermal Engineering 31, 3938–3945.

[16] Jradi M., Gillott M., Riffat S., 2013. Simulation of the transient behaviour of encapsulated organic and inorganic phase change materials for low-temperature energy storage. Applied Thermal Engineering 59, 211–222.

[17] Zhang H.L., Baeyens J., Degrève J., Cáceres G., Segal R., Pitié F., 2014. Latent heat storage with tubular-encapsulated phase change materials (PCMs). Energy 76, 66–72.

[18] Elmozughi A.F., Solomon L., Oztekin A., Neti S., 2014. Encapsulated phase change material for high temperature thermal energy storage – Heat transfer analysis. International Journal of Heat and Mass Transfer 78, 1135–1144.

[19] Solomon L., Elmozughi A.F., Oztekin A., Neti S., 2015. Effect of internal void placement on the heat transfer performance – Encapsulated phase change material for energy storage. Renewable Energy 78, 438–447.

[20] Sharma, A., Tyagi, V.V., Chen, C.R., Buddhi, D., 2009. Review on thermal energy storage with phase change materials and applications. Renewable and Sustainable Energy Reviews 13, 318-345.

[21] Hasnain S.M., 1998. Review on sustainable thermal energy storage technologies, Part I: heat storage materials and techniques. Energy Conversion and Management 39, 1127–1138.

[22] Jegadheeswaran S., Pohekar S.D., Kousksou T., 2012. Conductivity particles dispersed organic and inorganic phase change materials for solar energy storage-an exergy based comparative evaluation. Energy Procedia 14, 1.

[23] Haillot, D., Goetz, V., Py, X., Benabdelkarim, M., 2011. High performance storage composite for the enhancement of solar domestic hot water systems: Part 1: Storage material investigation. Solar Energy 85, 1021–1027.

[24] Velraj, R., Seeniraj, R.V., Hafner, B., Faber, C., Schwarzer, K., 1999. Heat transfer enhancement in a latent storage system. Solar Energy 65, 171–180.